NASA TECHNICAL TRANSLATION CSFC NO

NASA TT F-13,833

VACUUM RADIATION TEST OF THERMAL MOCK-UP OF INFRARED DETECTOR COOLING SYSTEM

F. Galzin

13 833

Translation of "Essai en vide rayonnement de la maquette thermique du système de refroidissement du detecteur I.R", National Center for Space Research, Brétigny, June 16, 1970
Report 70.CT.TA.TP/METEOSAT 0 492 28 pages

N72-14464 (NASA-TT-F-13833) VACUUM RADIATION TEST OF THERMAL MOCK-UP OF INFRARED DETECTOR COOLING SYSTEM F. Galzin (NASA) Jan. 1971
Unclas 41 p CSCL 14B
12345 G3/14
FACILITY (NASA CR OR TMX OR AD NUMBER) (CATEGORY)

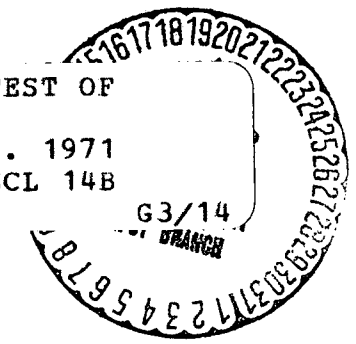

NATIONAL AERONAUTICS AND SPACE ADMINISTRATION
WASHINGTON, D.C. 20546 JANUARY 1971

Reproduced by
NATIONAL TECHNICAL
INFORMATION SERVICE
Springfield, Va. 22151

CENTRE NATIONAL D'ETUDES SPATIALES

CENTRE SPATIAL DE TOULOUSE

Brétigny, 16 June 1970

DIVISION "TECHNIQUES AEROSPATIALES"

70.CT.TA.TP/METEOSAT O. 492

Editor : F. Galzin

Department Chief : JP Delpont

DISTRIBUTION

B. ESTADIEU	.....	1 copy
H. FELIX	.....	1 copy
J. BRETON	.....	1 copy
R. ANGRAND	.....	1 copy
PR/AM	.....	1 copy
CT/SL	.....	1 copy
TA/TP	.....	10 copies
B.D.P.	.....	3 copies
LMD (M.SIROU)	..	1 copy

M E T E O S A T

VACUUM RADIATION TEST OF THERMAL MOCK-UP OF INFRARED DETECTOR COOLING SYSTEM

TABLE OF CONTENTS

1. Test Goal

2. Test Equipment
   2.1. Description of the model
   2.2. Cryogenic screen

3. Measurement Points
   3.1. Solar flux
   3.2. Temperatures
      3.2.1. Model
      3.2.2. Cryogenic screen

4. Development of Test

5. Data from the Thermal Model
   5.1. Thermooptical characteristics
   5.2. Radiative couplings
   5.3. Galvanic couplings

6. Test Results and Comparison With Calculations
   6.1. Results
   6.2. Discussions
      6.2.1. Measured temperatures
         6.2.1.1. Version I
         6.2.1.2. Version II
      6.2.2. Comparison with calculations

7. Conclusion

VACUUM RADIATION TEST OF THERMAL MOCK-UP OF INFRARED DETECTOR COOLING SYSTEM

ABSTRACT. Vacuum radiation tests in the METEOSAT program were carried out in a mock-up and demonstrated the feasibility of a passive thermal control for the infrared detector of the METEOSAT satellite in the case of reversal of the satellite. Description of mock-up provided. Test results are given in detail and compared with predicted results.

1. Test Goal

/3*

A mock-up was produced for a test whose goal was to:

demonstrate the feasibility of a passive thermal control for the infrared detector of the METEOSAT satellite in the case of reversal of the satellite;

demonstrate the validity of calculations carried out for several versions of the mock-up.

2. Test Equipment

The test was carried out in the SIMDIA simulator of SOPEMEA. It is a test involving vacuum-radiation.

2.1. Description of the mock-up

The mock-up, whose general drawing is provided as an annex (Chart I) includes:

an adapter made of AU4G allowing fastening of the mock-up proper on a thermal barrier which is itself fastened on the rotating arm of the simulator;

---

* Numbers in the right margin indicate pagination in the foreign text

a lower plate made of AU4G which is a ring 2 mm thick and whose inside and outside diameters are respectively equal to 560 and 895 mm. This part includes a stiffener at its periphery;

a central cylinder made of AU4G which is 2 mm thick with a 560 mm inside diameter and a 166 mm height;

an outside cylinder (AU4G) whose dimensions are as follows: thickness 1 mm, diameter 900 mm, height 179 mm;

an upper plate (AU4G) which appears in the shape of a ring 2 mm thick and with inside and outside diameters respectively equal to 34 and 895 mm. It includes a stiffener at its periphery;

the window of the detector, made of AG3, which is a truncated cone 1 mm thick whose semiangle at the vertex is equal to 30° and whose height is 12 mm. This window is glued on using araldite to the inside circle of the upper plate;

an outside screen, made of AU4G, in the shape of a truncated cone (thickness 1 mm, outside diameter = 975 mm, height 141 mm) is fastened on the outside cylinder and the upper plate stiffener by means of 8 clamps (length 21 mm, width 10 mm) and a screw with a 3 mm diameter. It is intended to eliminate solar /4 inputs to the upper part of the mock-up in certain versions;

an insulating carrier made of noryl ensuring connection between the structure and the radiating stages. It rests on the upper plate by means of 8 lugs. Fastening is ensured by 8 bolts with a 4 mm diameter;

a circular metal mask (AG3) 1 mm thick is fastened under the insulating carrier by 4 nylon bolts with a diameter of 4 mm. Its role is to limit the radiative exchanges between the insulating carrier and the first radiative stage;

a first radiative stage which, according to the version, is either made of AG3 or Makrolon. In the first case, its thickness is equal to 1 mm and, in the second case, it is 3 mm. In both cases, it appears in the shape of a ring with a 19 mm inside diameter and a 522 mm outside diameter;

a second radiative stage which is a disk with a 440 mm diameter. Depending on the case, it is made of AG3 and 1 mm thick or else made of Makrolon and 3 mm thick. This second radiative stage is connected to the

first one by means of 4 nylon screws with crosspieces made of Makrolon (diameter = 15 mm, height = 4 mm);

the detector cylinder made of AG3 (diameter = 15 mm, thickness = 1 mm, height = 25 mm) which is glued, using araldite, at the center and under the second radiative stage;

an inside screen in the shape of a truncated cone made of AG3 (thickness = 1 mm, inside diameter = 566 mm, outside diameter = 600 mm, height = 53 mm). It enables, depending on the version, protection of the second radiative stage from direct solar radiation or limiting its radiative exchanges with the outside screen;

the superinsulation entirely covering the upper plate. It is made up of aluminized mylar foils stuck on at various points using araldite and connected up in pairs, each pair consisting of one flat foil and one crimped foil. The part of the superinsulation located under the radiative stages includes 10 pairs of foils whereas the other part only contains 8.

For this test, 4 versions of the mock-up were planned:

Version 1: metal radiative stages, no outside screen;
Version 2: metal radiative stages, with outside screen;
Version 3: insulating radiative stages, without outside screen;
Version 4: insulating radiative stages, with outside screen.

2.2. Cryogenic screen /5

Since the level of temperature to be reached in the second radiative stage is on the order of 80° K, it was absolutely necessary to couple, during the test, this stage with a screen capable of being kept at a temperature less than 30° K.

An optimization study of this cryogenic screen (Memorandum 69/CT/TA/TP/METEOSAT/0.091) allowed specification of its dimensions.

This screen is a disk with a 900 mm diameter and cooled by gaseous helium. It is fastened on the simulator arm in an attitude such that its front surface is parallel to the first radiative stage and located at a distance of 18 cm from the latter.

It is supplied by a type PGH-105 cryogenerator. The screen was painted black on its front surface ($\varepsilon = 0.87$). Its other surfaces were metallic and polished so as to limit radiative exchanges with the tank.

3. Measurement Points

3.1. Solar flux

During the test, the mock-up has its axis in the working plane (plane 2500). In order to avoid a large thermal load on the cryogenic screen, the solar beam is occulted in such a manner that only the mock-up receives the flux.

The calibration of the solar flux was carried out before the test proper and the lights were regulated so as to obtain 140 mW/cm^2 in the working plane.

The 104 points where the measurements and flux values were made are shown on Figures 2 to 5.

The positioning of the points is provided by the following figure:

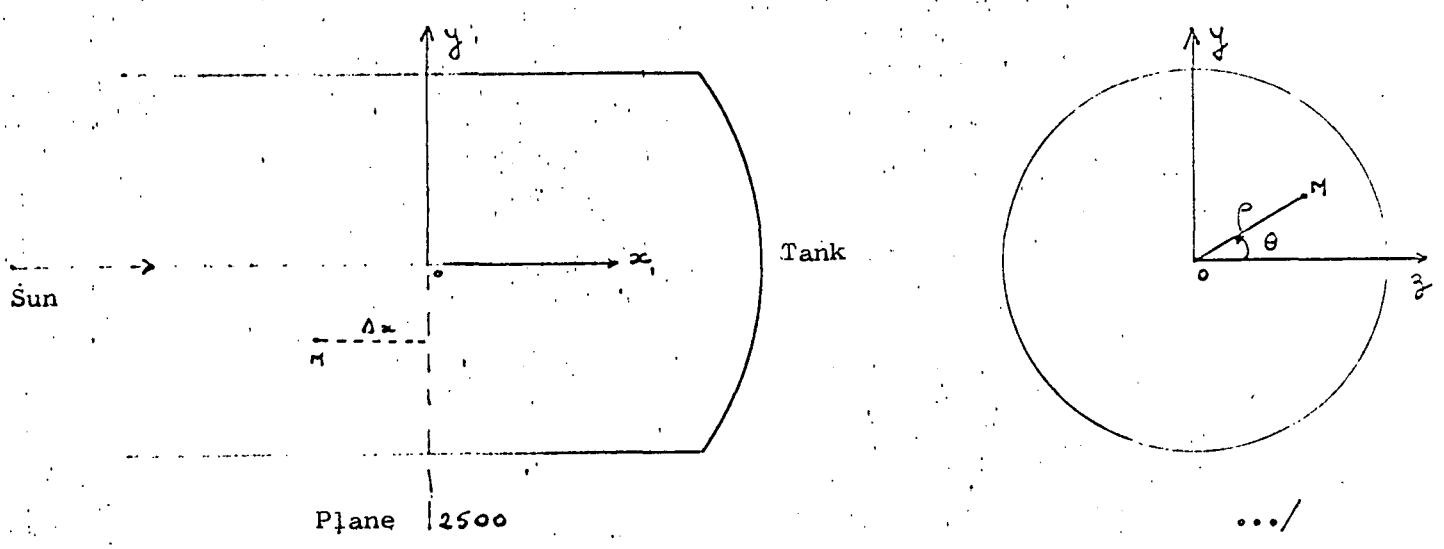

.../

3.2. Temperatures /6

3.2.1. Mock-up

Forty-two Cromel-Alumel thermocouples (diameter = 8/100th mm), distributed as 2 strands of 16 and 1 strand of 10, were either stuck or scotch-taped on at different points of the mock-up. The location of these thermocouples is provided in the general drawing (Chart 1) and on the detailed Figures 6 and 7.

As a safety precaution during changing of the radiative stages in order to go from the metallic version to the insulating version, two groups of thermocouples (1 to 7 and 8 to 14) were arranged redundantly. In the case where the outside screen is removed, thermocouples 30 and 31 are placed on the superinsulation. All thermocouples were calibrated on a preliminary basis at 3 points: 0° C, one point at -50° C, and one at -196° C in liquid nitrogen.

3.2.2. Cryogenic screen

On the surface of the cryogenic screen facing the mock-up, the 8 cryosensors (type TG-100) are arranged in special recesses. They allow measurement of temperatures going from 1 to 400° K with good precision (sensitivity 1.1 mV/° K at 20° K).

4. Development of Test

The total duration of the test was two weeks and 3 different versions of the mock-up were tested. Before each thermal balance, the following operations were carried out:

hooking the mock-up on the thermal barrier of the attitude simulator. The axis of the mock-up is in the working plane. The angle between the axis of the solar beam and that of the mock-up is equal either to 0° (i = 0°), or to 3° (i = 3°), the case in which the solar beam enters the inside of the outside cone;

closing the tank;

commencing operation of the cryogenic enclosure;

regulation of the lights in order to bring the solar flux up to

its nominal value;

regulation of electrical power dissipated in the thermal barrier of the attitude simulator so as to produce approximately 25° C on the cylinders of the mock-up;

commencing operation of the helium cryogenic screen. /7

In all cases, the rotation rate of the revolving arm was 6 rpm.

In this way, a first stage was achieved from the very first for Version I with i = 0°. Given the results obtained, it was decided not to carry out the test i = 3° for this same version. Following return to ambient conditions and opening of the tank, the outside screen was fastened on the mock-up. The test then had to be interrupted owing to a breakdown of light and thermal barrier. After repair, two thermal balances were successively achieved for Version 2 with i = 3° and i = 0°. Following return to ambient conditions and opening of the tank, the metal radiative stages of the mock-up were replaced by the insulating stages (Version 4). For this version, it was not possible to completely reach thermal balance with i = 0° owing to lack of time. Figures 8 and 9 show the development of the test and temperature levels reached during the latter.

5. Data from the Thermal Model

5.1. Thermooptical characteristics

A thermal model of the mock-up was produced for Versions I and 2. It includes 24 nodes in Version 1 and 25 in Version 2 (outside screen). In both cases, an additional node has been added representing the thermal barrier. Table 1 shows the nomenclature of the nodes, their coatings and thermooptical characteristics of the external nodes.

TABLE 1. NOMENCLATURE AND CHARACTERISTICS OF THE NODES

No. of the node	Designation	Coating	α	ϵ
1	Adapter	Black epoxy paint	0.96	0.87
2	Lower plate	"	0.96	0.87
3	Outside cylinder	"	0.96	0.87
4	Central cylinder	"		
5	Ring of the upper plate included between the 2 cylinders	"		
6	Outside screen	Aluminized TLH foil stuck on internal surface; white silicone paint on external surface	0.14 * / 0.22	0.04 * / 0.83
7	Part of the upper plate closing the central cylinder + + detector window	Black epoxy paint except window (gilding)		
8	Detector cylinder	Electrolytic gilding		
9	External surface of the superinsulating ring resting on node 5	Aluminized mylar	0.13	0.085
10	External surface of the superinsulating ring resting on node 7	"		
11	Mask	Electrolytic gilding		
12	Part of the insulating carrier	Internal surface: plain noryl External surface: white silicone paint		
13	"	"		
14	"	"		
15	"	"	0.22	0.83
16	"	"	0.22	0.83
17	"	"	0.22	0.83
18	"	Same + black epoxy paint on the surface with numbered radiative stages	0.22	0.84 (mean)
19	"	Internal surface: plain noryl External surface: black epoxy paint	0.96	0.87
20	"	"	0.96	0.87
21	"	"	0.96	0.87
22	"	Coarse noryl		
23	Inside screen	Internal surface: electrolytic gilding External surface: white silicone paint	0.25 * / 0.22	0.04 * / 0.87
24	First radiative stage	Electrolytic gilding everywhere except ring facing space directly: black epoxy paint	0.96	0.87
25	Second radiative stage	Internal surface: electrolytic gilding External surface: black epoxy paint	0.96	0.87
26	Thermal barrier	AU4G + teflon belt		$\sim$ 0.1

Footnote for Table on the preceding page

* The mean coefficients of absorption and transmission for nodes 6 and 23 are as follows:

node 6 :	$\bar{\alpha} = 0.22$	,	$\bar{\epsilon} = 0.435$	for i = 0°
	$\bar{\alpha} = 0.208$	,	$\bar{\epsilon} = 0.435$	for i = 3°
node 23 :	$\bar{\alpha} = 0.22$	,	$\bar{\epsilon} = 0.44$	

The cutting into nodes of the insulating (noryl) ring is shown in Figure 10.

5.2. Radiative couplings

All radiative couplings were calculated using the RADIOS program. More particularly, the exchanges between the black epoxy-painted ($\epsilon = 0.87$) cryogenic screen and the nodes of the mock-up facing it were calculated by means of this program by introducing a black fictitious node ($\epsilon = 0.9999$) in the shape of a truncated cone, supported, on one hand, by the mount of the cryogenic screen and, on the other hand, either by the greater periphery of the outside screen in the shape of a truncated cone (node 6) in the case of Version 2, or on the periphery of the superinsulation (node 9) in the case of Version 1.

5.3. Galvanic couplings

The galvanic couplings between metallic nodes were calculated by the usual methods.

The couplings between the metallic nodes and the external superinsulation surface (C_{5-9} and C_{7-10}) were calculated by taking an equivalent conductance of:

$1.5.\ 10^{-6}$ W/cm^2 °K for 10 pairs

$2.8.\ 10^{-6}$ W/cm^2 °K for 8 pairs

Finally, the conductances between 2 nodes of which at least one is made up by noryl were calculated by taking into account the variation of the thermal conductivity of this insulating substance as a function of temperature. The curve $\lambda noryl = f\ (t°)$ shown in Figure 11 was produced experimentally.

6. Test Results and Comparison With Calculations

6.1. Results

Tables 2, 3, and 4 show the temperatures measured and the temperatures calculated for the 3 thermal balances achieved during the test:

Version 1, $i = 0°$

Version 2, $i = 0°$

Version 2, $i = 3°$

Each table includes: /10

the temperatures measured. When several temperatures are given for one node, their order corresponds to that used for the thermocouples starting with the one with the lowest number;

the temperatures of each node calculated under the specific test conditions;

the temperatures of each node calculated by assuming the mock-up to be in space (elimination of cryogenic screen and tank).

TABLE 2. TEMPERATURES AT BALANCE /11

Version 1 - i = 0°

No. of node	Measured temperatures	Calculated temperatures	
		Under test conditions	In space
1	49,0 ; 23,4	32,1	31,4
2	12,7	18,4	17,6
3	32,9 ; 33,2	33,9	33,2
4	23,2 ; 24,9	27,2	26,5
5	26,2	28,7	28,0
7	26,8 ; 26,7	28,4	27,7
8	-139,2 ; -154,1 *	-163,0	-171,1
9	-1,9 ; - 31,2 * -22,1* ; 30,7 (TC 30 & 31)	- 91,6	- 93,6
10	-67,8 ; - 72,4 ; - 45,3	- 69,1	- 70,7
11	- 93,3	- 88,5	- 90,9
12		16,8	16,0
13	- 24,4	- 1,8	- 2,7
14		- 15,7	- 16,8
15	- 26,8	- 30,2	- 31,4
16	- 33 ; - 25,4	- 41,3	- 42,6
17		- 50,9	- 52,4
18	- 41,4	- 61,0	- 62,6
19	- 56,7	- 66,8	- 68,5
20		- 73,2	- 75,0
21	- 63,2 ; - 66,6	- 78,5	- 80,5
22	- 64,7	- 88,6	- 91,1
23	- 35,3	- 48,1	- 49,6
24	- 128,5 ; - 126,4 ; - 126,9 - 128,5 ; - 128,6 ; - 128,8	-124,9	-128,6
25	- 165,0 ; - 165,4 ; - 165,8 - 165,4 ; - 165,1 ; - 166,0	- 163,1	-171,2
26		34,8	34,1

* Measurement in error (cf. Paragraph 6.2.1.1)

TABLE 3. TEMPERATURES AT BALANCE /12

Version 2 - i = 0°

No. of node	Measured temperatures	Calculated temperatures	
		Under test conditions	In space
1	64,2 ; 32,4	39,7	38,9
2	18,4	20,0	19,2
3	33,8 ; 31,0	31,8	31,0
4	28,7 ; 29,8	29,3	28,5
5	30,0	27,3	26,5
6	- 16,2 ; - 23,9	- 19,9	- 20,8
7	32,4 ; 34,4	29,9	29,1
8	- 123,5 ; - 142,2 *	- 170,1	- 178,6
9	- 119,2 ; - 104,9	- 99,5	- 101,9
10	- 98,3 ; - 105,6 ; - 98,7	- 85,6	- 87,3
11	- 121,4	- 115,0	- 118,1
12		10,2	9,2
13	- 77,1	- 16,4	- 17,5
14		- 36,4	- 37,6
15	- 65,3	- 57,2	- 58,6
16	- 89,3 ; - 70,4	- 73,0	- 74,7
17		- 85,5	- 87,5
18	.....	- 96,5	- 98,7
19	- 115,7	- 101,1	- 103,5
20		- 105,6	- 108,2
21	- 101,7 ; - 105	- 108,7	- 111,4
22	- 107,9	- 115,1	- 118,2
23	- 140,2	- 131,3	- 135,1
24	(- 143,4 ; - 142,7 ; - 142,6 - 143,5 ; - 143,5 ; - 143,8)	- 140,5	- 145,0
25	(- 170,6 ; - 170,9 ; - 171,0 - 170,4 ; - 171,1 ; - 171,3)	- 170,2	- 178,7
26		45,0	44,3

* Measurement in error (cf. Paragraph 6.2.1.1)

TABLE 4. TEMPERATURES AT BALANCE

Version 2 - i = 3

No. of node	Measured temperatures	Calculated temperatures	
		Under test conditions	In space
1	64,0 ; 30,9	38,5	37,7
2	16,4	19,9	19,1
3	36,1 ; 32,9	32,5	31,7
4	27,1 ; 27,6	29,1	28,3
5	27,5	27,6	26,8
6	- 16,5 ; - 24,0	- 14,7	- 15,5
7	31,0 ; 32,9	29,7	28,9
8	- 122,4 ; - 137,4 *	- 169,9	- 178,5
9	- 119,1 ; - 103,6	- 99,2	- 101,6
10	- 97,1 ; - 104,2 ; - 98,2	- 85,5	- 87,2
11	- 118,6	- 114,7	- 117,9
12		10,5	9,5
13	- 77,7	- 16,1	- 17,2
14		- 36,1	- 37,4
15	- 65,6	- 56,9	- 58,3
16	- 89,5 ; - 70,4	- 72,7	- 74,4
17		- 85,2	- 87,2
18	.....	- 96,2	- 98,4
19	- 114,8	-100,8	-103,2
20		-105,3	-107,9
21	-103,2 ; - 104,6	-108,4	-111,2
22	- 107,5	-114,8	-118,0
23	- 139,4	-130,6	-134,5
24	-140,9 ; -140,3 ; -140,6 -141,1 ; -140,8 ; -141,6	-140,3	-144,8
25	-168,5 ; -168,3 ; -168,8 -168,1 ; -168,9 ; -168,6	-170,0	-178,6
26		43,9	43,1

* Measurement in error (cf. Paragraph 6.2.1.1)

Insofar as Version 4 is concerned, the temperatures measured at the end of the test are shown in Table 5. /14

The discrepancy between the forecast results and those produced for this version is such that the thermal model itself must be blamed. Indeed, the simplified thermal model used during the definition calculations of the mock-up suggested a gain of 5 to 10° K with respect to Version 2 with the coldest point located at the center of the radiator. Now, the test results have shown that the hottest point was in the center and the coldest point on the periphery.... The only possible explanation is the poor quality of the thermal model, more particularly at the level of interstage fastenings. The setting up of a precise thermal model would require the sectioning of the insulating part into a very great number of nodes and long and complicated calculations incompatible with the present working load of the department.

TABLE 5. MEASURED TEMPERATURES AT BALANCE

Version 4 - 1 = 0

No. of the node	Temperature	No. of the node	Temperature	No. of the node	Temperature
1	66,0 ; 32,2	10	-77,1;-97,0;-93,9	19	- 110,8
2	17,0	11	- 103,1	20	
3	35,3 ; 32,1	12		21	-103,4;-105,1
4	28,0 ; 28,4	13	- 18,0	22	-111,3
5	27,8	14		23	-140,8
6	-16,8 ; - 19,7	15	- 61,7	24	-127,5;-141,6 - 141,7
7	31,8 ; 32,4	16	- 88,4 ; - 66,1		-127,3;-141,5 - 144,1
8	- 140,0 ; - 172,5 *	17			
9	- 120,8 ; - 109,2	18	.....	25	-146,1;-170,9 -175,8 -145,9;-170,0 -176,3
				26	

6.2. Discussions

/15

6.2.1. Measured temperatures

6.2.1.1. Version 1

After opening the tank we ascertained that the heads of thermocouples 8, 21, and 30 were not stuck directly to the surface of the node with mylar for the remainder of the test. On the other hand, since it was difficult to reach thermocouple 8, the only action possible was to try and attach it with scotch tape with no guarantee of the result. The results of the following tests show that measurements provided by this thermocouple are still erroneous.

The homogeneity of temperatures for nodes 3, 4, 7, 24 and 25 was noted.

The deviation between the temperatures provided by the two thermocouples of node 9 (surface of the external superinsulation) is explained by the fact that its surface was not perfectly flat and some parts probably received solar flux. As far as node 10 is concerned (surface of the internal superinsulation), the temperature provided by thermocouple 28 is quite different from the two others. It appears that this may be owing to the fact that it is located near the insulating ring whose temperatures are much higher than those of the two other thermocouples of node 10. (This edge effect is always troublesome in superinsulating coverings).

6.2.1.2. Version 2

During the whole test of this version, thermocouple 23 (node 18) was nonoperational.

The difference between temperatures provided by the two thermocouples of node 6 is explained by the heterogeneity of the solar flux.

The magnitude of the lateral thermal gradient in the insulating ring was noted.

There is no considerable difference in temperature levels between tests $i = 0°$ and $i = 3°$, tending to prove that the radiative insulation is good.

6.2.2. Comparison with calculations /16

A comparison of measured temperatures and calculated temperatures under test conditions shows:

that there is a good agreement between measurement and calculation for the metallic nodes except for nodes 23 (inside screen) and 8 (detector cylinder);

that the forecast of temperatures of the insulating ring was not very good. However, in order to have more precision, it would have been necessary to cut this ring into a greater number of nodes, since the longitudinal and transverse gradients in a section have turned out to be great at some locations;

that there is not a good agreement in temperatures recorded for the superinsulation. The causes for error in latter measurements are many. There are, for example, edge effects causing lateral leakage, warping of the mylar foil, the difficulty of experimentally measuring with precision the apparent conductivity of coverings, etc. In spite of this, it was ascertained that the effectiveness of the superinsulation was greater than expected.

The deviation in temperature recorded between calculation and test with node 23 comes from the poor prediction of node 9 and the insulating ring temperatures. Insofar as node 8 is concerned, it appears that the measurement itself should be blamed. Nevertheless, the temperature of this node is secondary, since the large temperature reading is that of the center of the second radiative carrier stage of the infrared detector.

Finally, the calculation carried out with the same thermal model in space reveals a gain of approximately 8° C over the temperature of the second radiative stage. This is owing, to a large part, to the overpressure from undesired reflections on the cryogenic screen.

7. Conclusions

The validity of the thermal model, updated after testing, has been demonstrated. Since the maximum temperature produced during the test on the detector did not exceed 105° K (in Version 2), the calculations made using this thermal model in actual space suggest a detector temperature not exceeding

95° K.

The feasibility of a passive cooling system of the detector is thereby demonstrated in the case where the satellite is reversed every six months. In addition, the existing version can be improved by use of a black paint with higher emissivity and more carefully finished specular metal coatings. /17

In the case where reversal is not planned, the design of the cooling system should be reexamined owing to the need for reducing the solar thermal inputs through a suitable baffle system. The feasibility of passive cooling of the detector under these conditions remains to be proven. It is probable that it will present great difficulties.

Calibration points for solar flux

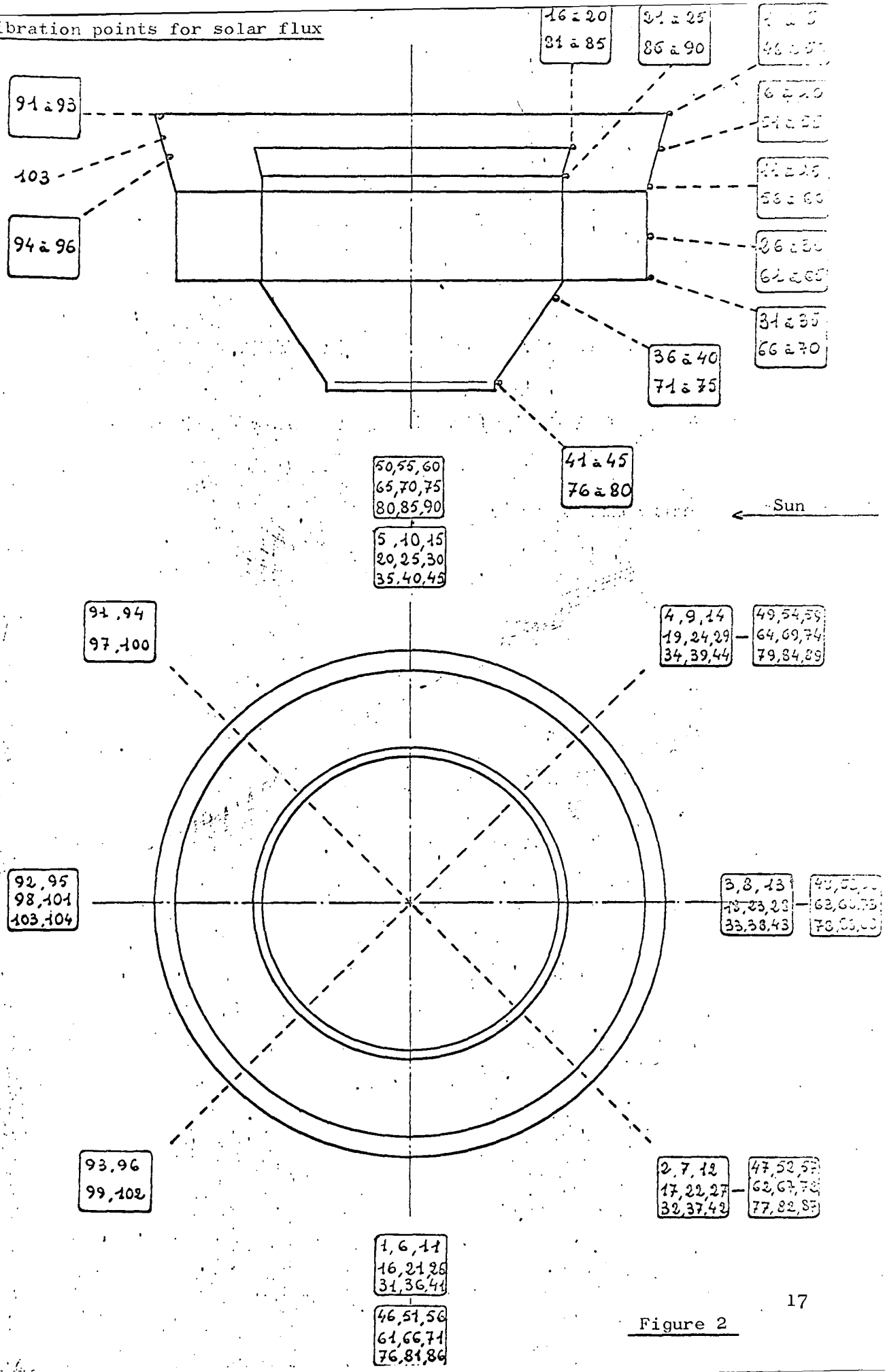

Figure 2

S.O.P.E.M.E.A. Technical Record Sheet

Order N°: B 2387 Matériel : Date : 13/2/70 Page 1

Test METEOSAT Machine : Opérator : Soucon

N°	Δx cm	ϕ cm	θ deg	mV	mW/cm²		N°	Δx cm	ϕ cm	θ deg	mV	mW/cm²
1	0	50,0	257,0	11,59	102		21	0	28,6	270	16,59	150
2	-42,2	26,8	245,3	14,85	134		22	-24,8	11,3	270	20,20	182
3	-28,7	11,2	180	11,85	106		23	-28,6	0	ind.	19,80	178
4	-42,2	26,8	114,6	10,97	99		24	-24,8	14,3	90	19,86	178
5	0	50,0	103,0	4,86	24		25	0	28,6	90	15,77	142
6	0	47,3	263,9	13,52	121		26	0	46,3	283,7	14,05	126
7	-20,7	24,0	257,8	22,79	205		27	-39,0	25,0	296,1	22,69	205
8	-47,0	5,1	180,8	23,02	207		28	-45,0	11,0	0	23,87	215
9	-40,7	24,0	102,2	21,77	196		29	-39,0	25,0	63,9	21,67	195
10	0	47,3	96,1	9,82	79		30	0	46,3	76,3	9,39	85
11	0	45,0	272,5	14,08	126		31	0	49,2	294	13,25	120
12	-39,0	22,6	275,0	22,80	205		32	-39,0	30,1	301,6	21,93	198
13	-45,0	2,0	0	22,90	206		33	-45	20,0	0	24,39	220
14	-39,0	22,6	85,0	21,85	197		34	-39,0	30,1	48,4	20,35	163
15	0	45,0	87,5	10,41	94		35	0	49,2	66,0	7,32	65,5
16	0	30,4	260,2	16,35	147		36	0	34,4	310,9	16,23	146
17	-26,0	15,9	250,9	20,42	184		37	-22,5	26,0	330	19,22	172
18	-30,0	5,2	190,	19,95	179		38	-26,0	22,5	0	20,91	188
19	-26,0	15,9	109,1	19,97	179		39	-22,5	26,0	30	19,41	174
20	0	30,4	93,8	15,56	140		40	0	34,4	49,1	15,03	135

Reproduced from best available copy.

Calibration of solar flux

Figure 3

ϕ at center ϕ au centre 15,53 mV → 140 mW/cm².

S.O.P.E.M.E.A. Technical Record Sheet

Order N°: ..... Matériel : ..... Date : ..... Page 2

Test: METEOSAT Machine : ..... Opérator : .....

N°	N°s	Δx cm	ϕ deg	θ deg	mV	mW/cm²		N°s	Δx cm	ϕ cm	θ deg	mV	mW/cm²
1	41	0	41,8	333,0	14,89	134		60	0,1	45,0	87,5	10,63	96
2	42	-13,0	39,7	349,2	16,53	148		61	0,6	46,3	283,7	11,04	126
3	43	-15,0	39,0	0	16,37	148		62	-38,4	26,0	300	22,61	203
4	44	-13,0	39,7	10,8	15,77	142		63	-44,4	13,3	0	24,06	222
5	45	0	41,8	21,0	13,75	123		64	-38,4	26,0	60	21,34	192
6	2ème cas.							65	0,6	46,3	76,3	9,46	85,5
7	46	-0,6	50,5	256,0	10,49	124		66	1,0	49,2	292,9	13,33	120
8	47	-43,0	26,4	21,79	22,88	205		67	-37,9	31,5	314,2	21,50	194
9	48	-49,6	9,6	180	17,21	164		68	-43,5	22,3	0	24,16	218
10	49	-43,0	26,4	112,1	19,65	168	?	69	-37,9	31,5	45,7	19,85	179
11	50	-0,6	50,5	104	3,0	27	?	20	1,0	49,2	66,1	7,54	68
12	51	-0,3	47,3	263,9	13,61	122		21	1,2	34,4	310,8	16,18	146
13	52	-40,9	23,7	262,8	22,95	207		72	-21,3	27,0	331,2	19,73	177
14	53	-47,2	2,6	120	23,22	209		23	-24,9	23,7	0	20,60	185
15	54	-40,9	23,7	97,2	21,55	197		74	-21,3	27,0	28,8	19,32	174
16	55	-0,3	47,3	96,1	8,59	77		75	1,2	34,4	49,2	14,99	135
17	56	0,1	45,0	272,5	14,23	128		76	2,0	41,7	339,0	14,73	133
18	57	-37,7	22,9	270,1	23,94	207		77	-40,9	20,3	349,3	16,03	144
19	58	-44,8	1,3	0	23,30	210		78	-43,9	39,7	0	16,06	144
20	59	-37,7	22,9	79,9	21,86	196		29	-40,9	20,3	10,2	15,04	135

Reproduced from best available copy.

Calibration of solar flux

Figure 4

19

S.O.P.E.M.E.A. — Technical Record Sheet

Order: N°: 20 — Matériel: — Date: — Page:

Test: METEOSAT — Machine: — Opérator:

N°	N°	Δx cm	ρ cm	θ deg	mV	mW/cm²
1	80	2,0	41,7	21,0	13,81	124
2	81	-0,3	30,4	260,2	16,47	149
3	82	-26,2	15,5	255,6	20,62	186
4	83	-30,2	3,6	180	20,16	182
5	84	-26,2	15,5	104,4	20,15	182
6	85	-0,3	30,4	95,8	15,83	142
7	86	0	28,6	270	17,36	156
8	87	-24,8	14,4	275,2	20,67	186
9	88	-28,6	1,5	0	20,27	183
10	89	-24,8	14,4	84,8	20,30	186
11	90	0	28,6	90	16,08	145
12	91	41,7	29,4	120,4	10,17	92
13	92	48,3	14,7	190	10,84	98
14	93	41,7	28,4	239,6	11,99	108
15	94	40,9	25,9	112,2	10,26	92
16	95	47,2	9,5	190	11,38	103
17	96	40,9	25,8	247,8	12,67	114
18	97	25,7	16,4	113,6	13,52	122
19	98	29,7	6,8	180	12,87	116
20	99	25,7	16,4	246,4	13,75	123

N°s	Δx cm	ρ cm	θ deg	mV	mW/cm²
100	25,1	15,1	104,2	13,56	122
101	28,9	3,5	180	12,83	115
102	25,1	15,1	255,8	13,68	123
103	47,7	11,9	180	12,84	115
104	29,3	5,3	183	12,84	115

Reproduced from best available copy.

Calibration of solar flux

Figure 5

ϕ at center excentre 15,71 mV → 141,5 mW

Centre National d'Etudes Spatiales

METEOSAT

Figure 6

Thermal Mock-Up

Location of the thermocouples

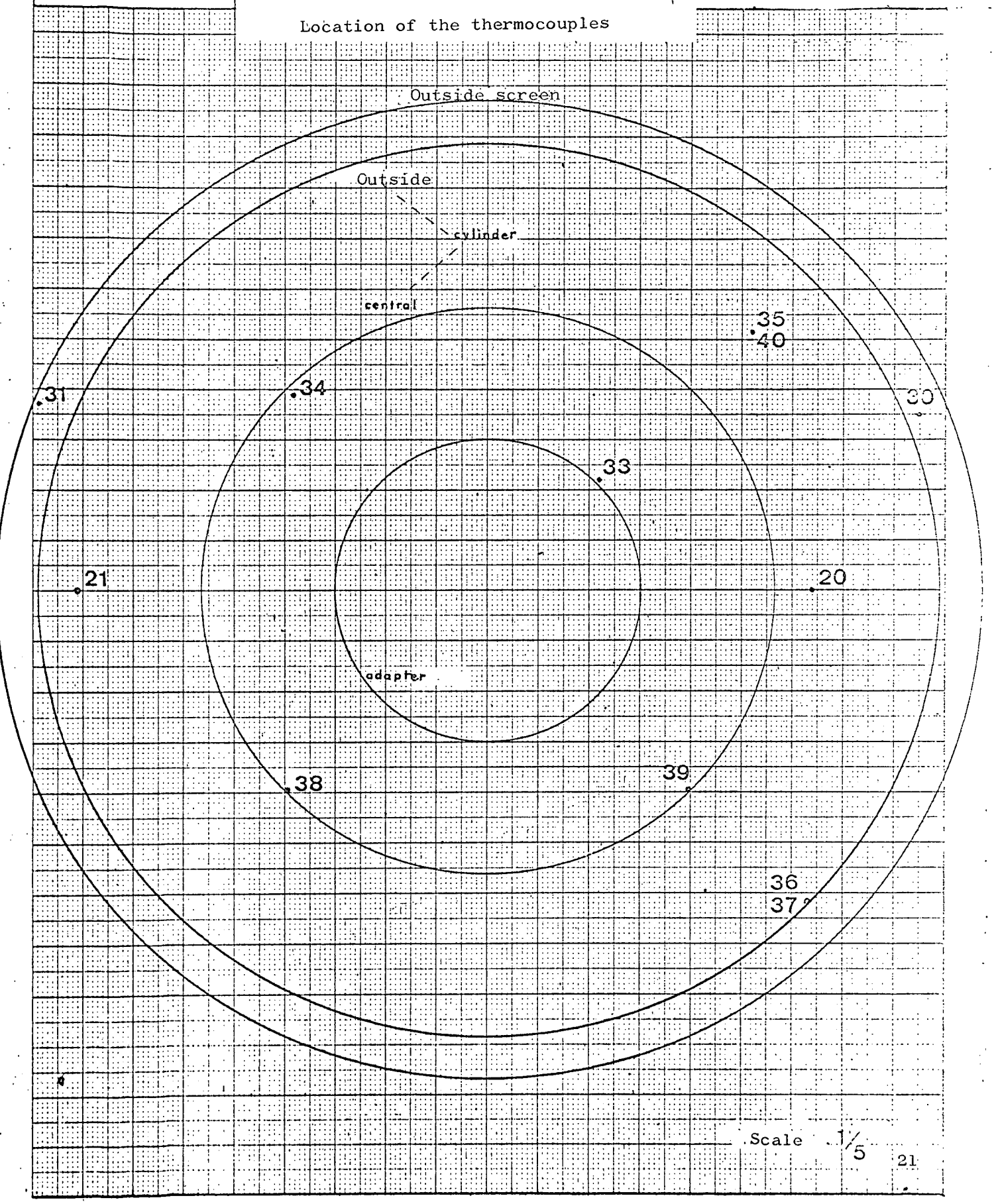

Scale 1/5

Centre National d'Etudes Spatiales

METEOSAT

Figure 7

Thermal Mock-Up

Location of the thermocouples

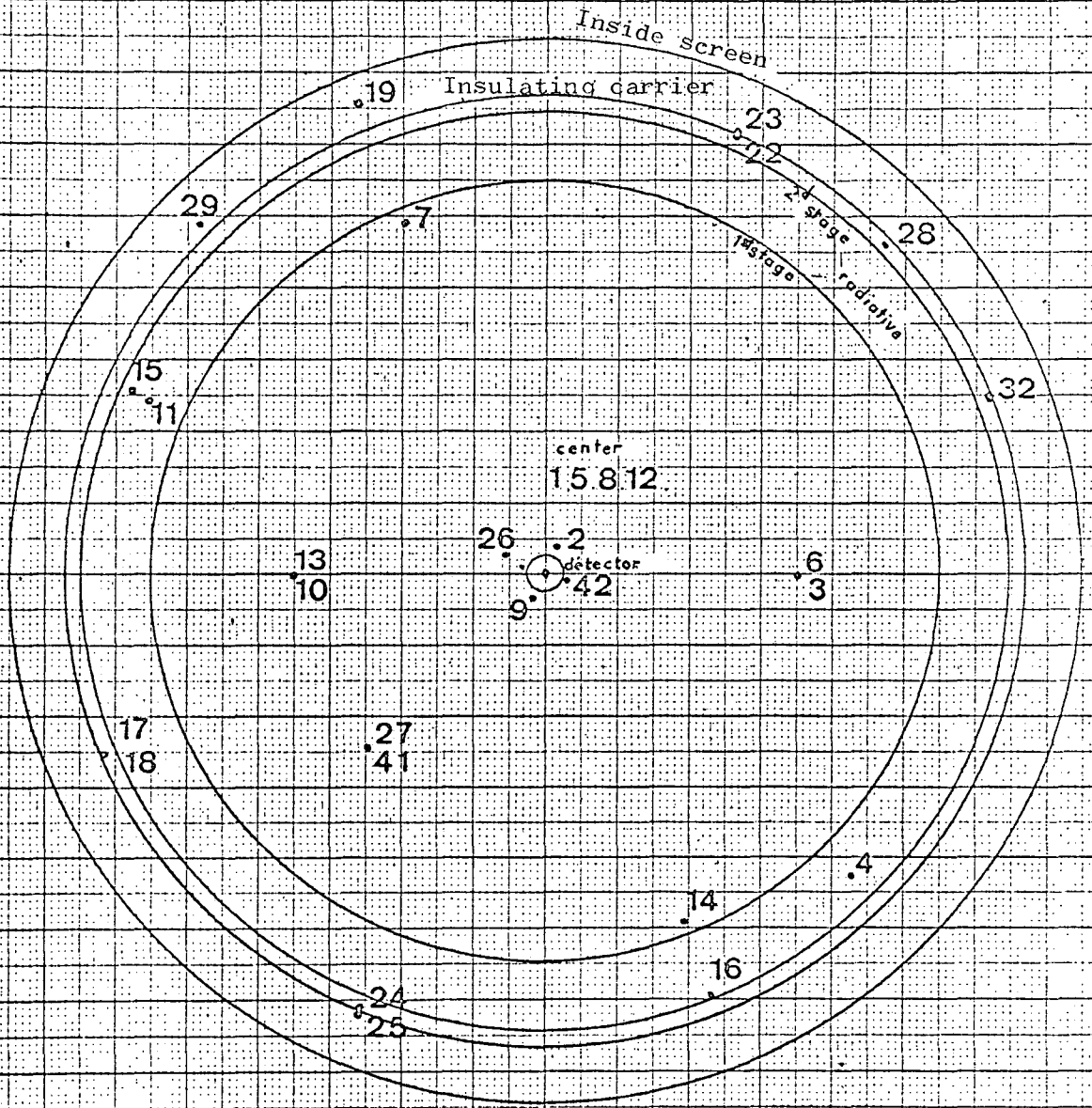

Scale: 1/4

Centre National d'Etudes Spatiales

DEVELOPMENT OF TEST

(Part 1)

Figure 8

FOLDOUT FRAME 2

NOT REPRODUCIBLE

THERMOCOUPLES

0-10 Black surface helium screen

3-5 Center of the 2d stage

5-10 One of the 4 master temperatures on the structure

FOLDOUT FRAME

NOT REPRODUCIBLE

Computing temperature (°C)

-100

-50

0°C

-50

-100

-150

-200

-250

Sun + Cold

CRYOGENERATOR

TC 5-10

Cryo failure

TC 3-5

Version 1 i = 0°

-1.5°C

TC 0-10

(Actual step 25 to 38°K)
voltage 1.465

Monday 16

Tuesday 17

Wednesday

8 17 24 8 17 24 8

Sun + Cold

TC 5-10

Sun breakdown
(one light)

Electric heating plate
(complete halt)

CRYO

TC 3-5

Version 2 i = 0°

TC 0-10

(Actual step 20 to 32°K)
voltage 1.480

Thursday 19

Friday 20

23

24 8 17 24 8 17 24

Computing date

Centre National d'Etudes Spatiales

DEVELOPMENT OF TEST

NOT REPRODUCIBLE

(Part 2)

Figure 9

FOLDOUT FRAME

THERMOCOUPLES

0-10 Black surface helium screen

3-5 Center } of the 2d stage
3-7 Periphery }

5-10 One of the 4 master temperatures on the structure

Computing temperature (°C)

100

50

0°C

-50

-100

-150

-200

-250

Normal reswitching in of computing temperatures

Control error (reversal of computing temperature TC)

Sun + Cold

CRYO

Tc 5-10

Tc 3-5

Version 2 L=3° L=6°

Tc 0-10

(Actual step 20 to 32°K) voltage 1.480

Monday 23 | Tuesday 24 | Wednesday 25

17 24 8 17 24 8 17

Sun + Cold

Restarting of cryogenerator after breakdown

Tc 5-10

Tc 3-5

Tc 3-7

Version 4 L=0°

Tc 0-10

(Actual step 20 to 32°K) voltage 1.480

24 | Thursday 26 | Friday 27

24 8 17 24 8 17 24

Computing date

FOLDOUT FRAME 2

Figure 10

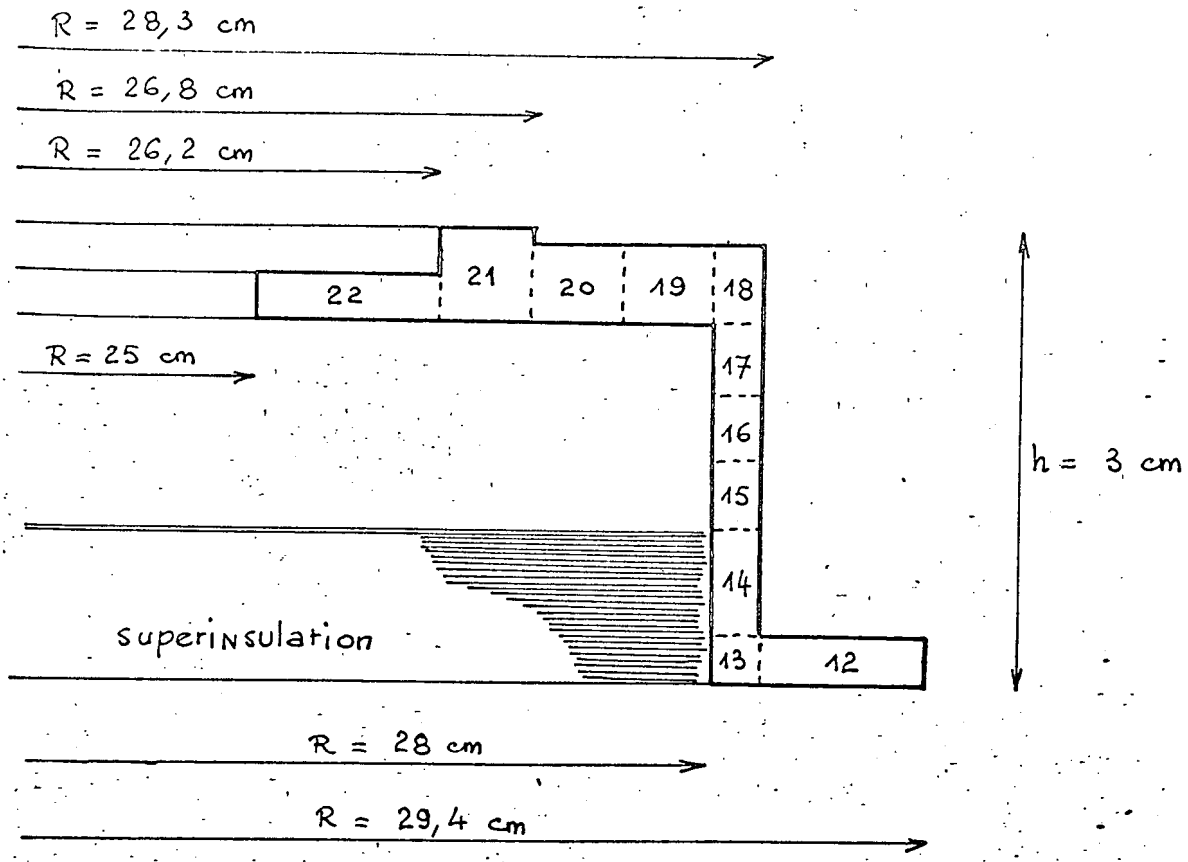

Cutting into nodes the rotating part made of noryl

Figure has 2/1 scale

Centre National
d'Etudes Spatiales

Figure 11

THERMAL CONDUCTIVITY OF NORYL

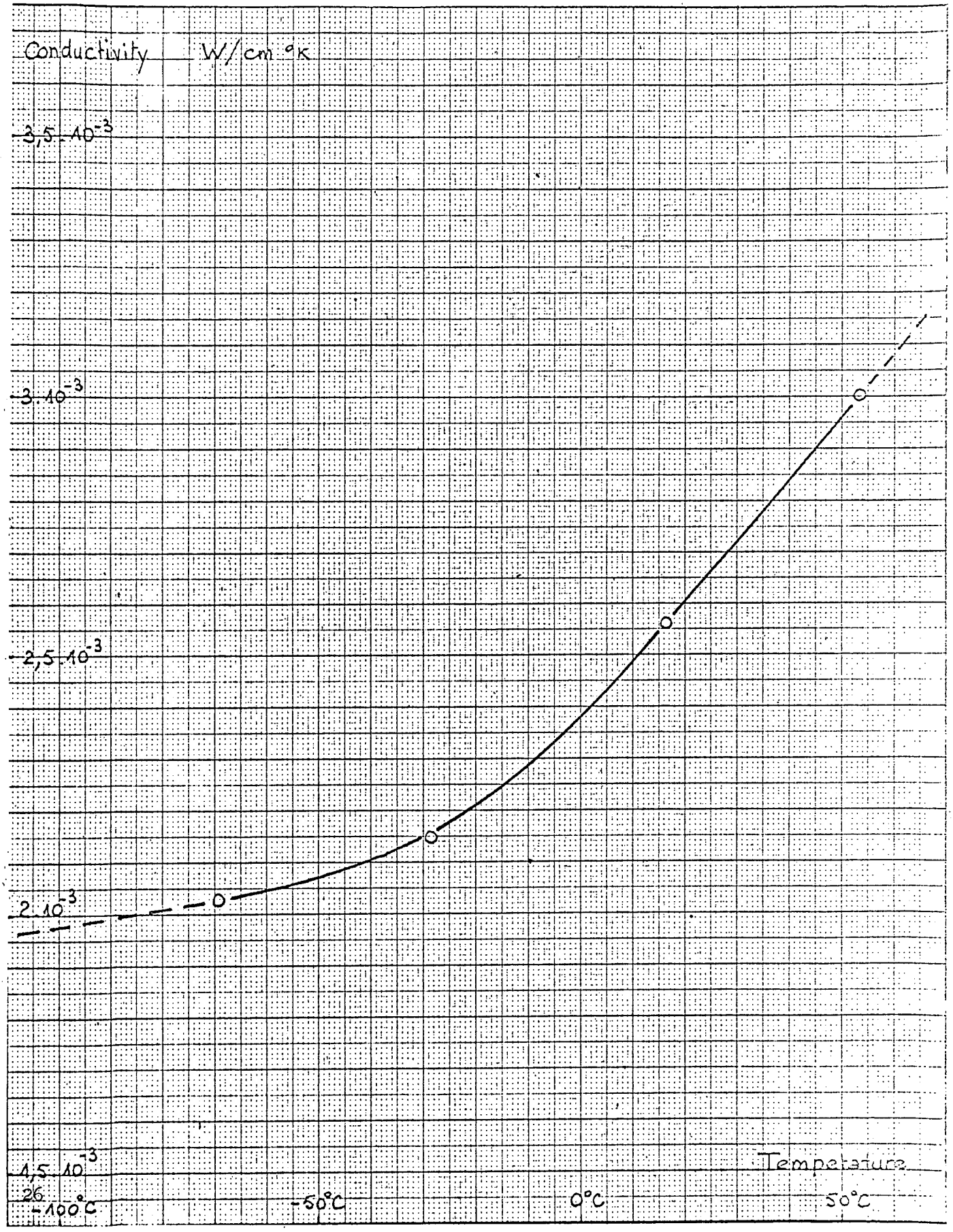

Page intentionally left blank